The proliferation of space objects is a rapidly increasing source of artificial night sky brightness

M. Kocifaj,[1,2][*] F. Kundracik,[2] J. C. Barentine,[3,4] S. Bará,[5]

[1]*ICA, Slovak Academy of Sciences, Dúbravská cesta 9, 845 03 Bratislava, Slovakia*
[2]*Department of Experimental Physics, FMPI, Comenius University, Mlynská dolina, 842 48 Bratislava, Slovakia*
[3]*International Dark-Sky Association, 3223 N. 1st Ave, Tucson, AZ 85710 USA*
[4]*Consortium for Dark Sky Studies, University of Utah, 375 S 1530 E, RM 235 ARCH, Salt Lake City, Utah 84112-0730 USA*
[5]*Departamento de Física Aplicada, Universidade de Santiago de Compostela, E-15782 Santiago de Compostela, Galicia, Spain*

ABSTRACT

The population of artificial satellites and space debris orbiting the Earth imposes non-negligible constraints on both space operations and ground-based optical and radio astronomy. The ongoing deployment of several satellite 'mega-constellations' in the 2020s represents an additional threat that raises significant concerns. The expected severity of its unwanted consequences is still under study, including radio interference and information loss by satellite streaks appearing in science images. In this Letter, we report a new skyglow effect produced by space objects: increased night sky brightness caused by sunlight reflected and scattered by that large set of orbiting bodies whose direct radiance is a diffuse component when observed with the naked eye or with low angular resolution photometric instruments. According to our preliminary estimates, the zenith luminance of this additional light pollution source may have already reached $\sim$20 μcd m^{-2}, which amounts to an approximately 10 percent increase over the brightness of the night sky determined by natural sources of light. This is the critical limit adopted in 1979 by the International Astronomical Union for the light pollution level not to be exceeded at the sites of astronomical observatories.

Key words: light pollution – methods: statistical – methods: data analysis

1 INTRODUCTION

Artificial satellites orbiting the Earth have been a concern of astronomers since the launch of the first such object, Sputnik 1, in 1957. As of 1 January 2021, some 3,372 satellites are in orbit (UCS 2021) along with many tens of thousands of pieces of space debris; we refer to both satellites and space debris here as "space objects."

The orbital altitudes of space objects range from a few hundred kilometres in the case of objects in Low-Earth Orbit (LEO) to beyond the 35,786-km height defining geosynchronous orbits. At such altitudes, space objects remain directly illuminated by sunlight as seen from the night side of the Earth; consequently, they appear in images obtained with ground-based telescopes as streaks of various lengths and apparent brightness depending on the orbital parameters of the objects. Because the streaks are often comparable to or brighter than objects of astrophysical interest, their presence tends to compromise astronomical data and poses the threat of irretrievable loss of information.

The number of space objects orbiting Earth is expected to increase by more than an order of magnitude in the next decade due to the launches of fleets of new, large 'constellations' of communications satellites. While astronomers can often plan observations around the presence of bright space objects in their telescopes' fields of view by predicting their apparent positions on the night sky using databases of orbital elements, the expected increase in the space object population significantly increases the probability that any particular observation will be affected by streaks. Hainaut at al. (2020) and Tyson et al. (2020) recently explored the expected impacts of large satellite constellations on both optical and near-infrared astronomical observations, finding that ultra-wide imaging exposures made with large survey telescopes will be most affected, with up to 40% of science exposures affected by streaks assuming the largest expected numbers of new satellites and an overall loss of $\sim$1% of science pixels.

To date there is little information in the literature as to the contribution of space objects to the diffuse brightness of the night sky, as opposed to the effect of discrete streaks that add systematic errors to astronomical data. While the
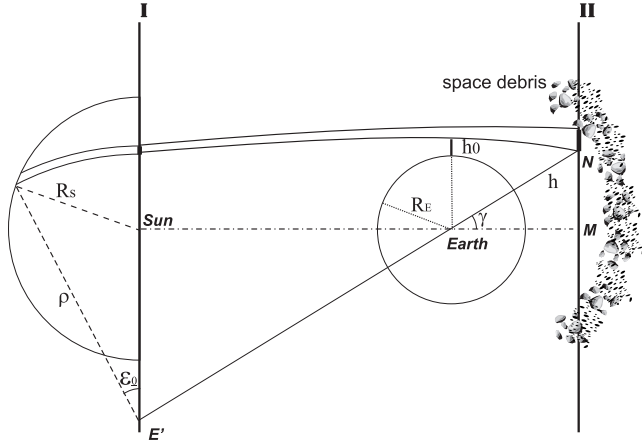

Figure 1. A simplified illustrative view of space debris orbiting the Earth and directly illuminated by sunlight. Planes I and II are for the Sun and the Earth, respectively, while the parameters used are described in the main text. The drawing is not to any particular scale.

night sky luminance signal due to sunlight reflected from space objects and propagating in the Earth's atmosphere is expected to be small, it is otherwise unknown how its contribution to diffuse night sky brightness (NSB) compares to natural sources of light in the night sky that ultimately determine the sky luminance over 'pristine' locations nearly devoid of anthropogenic skyglow, such as the sites of astronomical research observatories.

We decided to estimate the present-day diffuse NSB contribution from space objects, before the ongoing deployment of large communication satellite constellations increase in order to benchmark future NSB observations in these pristine places. In the current work, we describe the geometry of the situation and model the diffuse NSB specifically attributable to sunlight reflected from space objects, establishing lower limits for the space object contribution based on expectations for coming launches and the potential for orbital crowding to generate new sources of space debris.

This paper is organised as follows. We develop the requisite theory, establish the expected spectral radiance of space objects in the observer's zenith, and compute the zenith night sky luminance contribution from space objects in Section 2. We present the results of our calculations and discuss their implications in Section 3. Finally, we draw conclusions from this work and speculate on future prospects in Section 4.

2 SKY BRIGHTNESS DUE TO SPACE OBJECTS

Due to their high altitudes, objects in orbit around the Earth can be visible after the onset of astronomical night; i.e., for solar depression angles $\geq 18°$. For instance, objects at altitudes between 1000–2000 kilometres can be directly illuminated by sunlight and observed in the zenith even when the depression angle of the solar disc is 30-40°. The lower the minimum altitude of light rays, the more such rays diverge due to atmospheric refraction; see the quantity h_0 in Fig. 1. Depending on beam trajectory, the angle of refraction is 1′ at an altitude of 30 km, 10′ at $h_0 \approx 15$ km, and

approaches 1° for rays entering the lower troposphere (Link 1969). Satellites illuminated by such low rays are normally dark or even invisible because of exceptional atmospheric extinction of sunlight.

Since the deflection of the light beam is extremely low, most space objects orbiting the Earth are either directly illuminated by sunlight or disappear once they cross into the geometrical shadow of the Earth.[1] A few objects moving in a 'transition zone' between positions unaffected by the Earth's atmosphere and those obstructed by the Earth contribute negligibly to the diffuse brightness of the night sky, and thus are not considered in the following analysis. The transition zone is defined by the angle of refraction, which normally does not exceed 1°. The objects traversing the sky from the twilight region into the Earth's shadow are constantly illuminated by sunlight and seen in the visual field of 90° or more; thus, the number of objects in the transition zone is about 1% of all objects we can see in the night sky.

2.1 Spectral radiance

The spectral irradiance (W m^{-2} nm^{-1}) at a point N located at an altitude h above the Earth's surface is

$$E_\lambda(\gamma) = 2b_{0,\lambda} \int_{\gamma - R_S}^{\gamma + R_S} T_\lambda^{Ext}(\rho)\, \epsilon_0(\rho)\, d\rho \,, \qquad (1)$$

where $b_{0,\lambda}$ is the average radiance of the Sun (W m^{-2} nm^{-1} sr^{-1}), λ is the wavelength of radiation, γ is the angular distance measured from the centre of the Earth between the position of an illuminated object (in point N) and the centre of the Earth's shadow (in point M), R_S is the angular radius of the solar disc, ρ is the angular distance ranging from $\gamma - R_S$ to $\gamma + R_S$, and ϵ_0 is the maximum opening angle at an angular distance of ρ, i.e.,the angle between centre of solar disc and the limb (consult Fig. 1). The transmission coefficient T_λ^{Ext} characterizes attenuation of sunlight in the atmosphere due to extinction (see, e.g., Kocifaj and Horvath 2005). In the absence of the terrestrial atmosphere, or for high-altitude beams with $h_0 \gtrsim 60$ km (Link 1969), Eq. (1) reduces to

$$E_{0,\lambda} = 2b_{0,\lambda} \int_{\gamma - R_S}^{\gamma + R_S} \epsilon_0(\rho)\, d\rho \; = b_{0,\lambda}\pi R_S^2 \,, \qquad (2)$$

with πR_S^2 being the solid angle subtended by the solar disc in steradians.

Of all photons entering the point N, a small fraction is intercepted by space objects and redirected toward the Earth. The redirection is dominated by scattering in the case of debris objects smaller than or comparable to the wavelengths of visible light. For larger macroscopic objects to which the principles of geometric optics are applicable, direct reflection of light dominates the redirection. The amount of redirection is proportional to $E_{0,\lambda} \frac{P_\lambda(\theta)}{4\pi} k_\lambda(h)$, where $P_\lambda(\theta)$ is scattering phase function normalized to 4π, and θ is the scattering angle, i.e., the angle between the incident beam and the scattered beam. Conservation of energy requires that $\int \frac{P_\lambda(\theta)}{4\pi} d\omega = 1$, where $d\omega = 2\pi \sin(\theta) d\theta$ is the elementary solid angle.

---

[1] The geometrical shadow of the Earth neglects refraction effects from the terrestrial atmosphere.

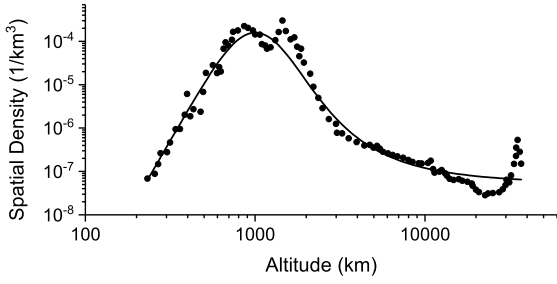**Figure 2.** Spatial density of space objects larger than 1 mm as a function of altitude. Dots are data published by Bendisch et al. (2004), while the solid line represents our fitted model.
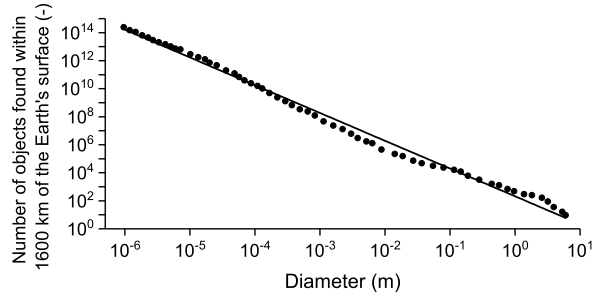

Figure 3. Logarithmic relationship between cumulative number and sizes of LEO objects. Dots are data published by National Research Council (1995) while the solid line is the analytic fit. The data shown are for objects within 1600 kilometres of the Earth's surface.

Artificial satellites and pieces of space debris have diverse shapes and are oriented randomly in the line of sight, scattering and reflecting light in a complex manner. However, the number of orbital objects is large, and statistical averaging over a large sample size yields results similar to those for equally sized spherical objects. Since most space objects are very large compared to the wavelengths of visible light, they scatter light strictly in the geometrical optics regime. The resulting optical signal therefore depends much more strongly on an object's geometric cross section rather than on its morphology.

The volume scattering coefficient $k_\lambda(h)$ can be computed from Mie theory (see, e.g., Hergert and Wriedt 2012) by treating a given object as a sphere of radius of r:

$$k_\lambda(h) = \pi \int_0^\infty r^2 n(r,h) \, Q_{\lambda,sca}(r) \, dr, \quad (3)$$

where $Q_{\lambda,sca}(r)$ is the scattering efficiency factor for an object of radius r illuminated by monochromatic light of wavelength λ. The function $n(r,h)dr$ is the number of objects of radius $r \rightarrow r + dr$ per cubic meter such that $n(r,h)$ is expressed in units of m^{-4}. For objects larger than the typical observational wavelengths $Q_{\lambda,sca} \approx 1$ to 2.

The spectral radiance due to the reflection of sunlight in all space objects in Earth orbit along the line of sight z, detected by an observer at ground level is

$$L_\lambda(z) = \frac{e^{-\tau_\lambda/\cos z}}{\cos z} E_{0,\lambda} \int_{h_1}^\infty \frac{P_\lambda(\theta)}{4\pi} k_\lambda(h) \, dh, \quad (4)$$

where τ_λ is the optical thickness of Earth's atmosphere, z is the zenith angle of observation, and h_1 is the minimum orbital altitude of space objects. The latter parameter is normally a few hundred kilometers (see Fig. 2), but the lower integration limit can also be asymptotically extended to $h_1 = 0$ km assuming that both the number density of space objects and $k_\lambda(h)$ approach zero near the Earth's surface. Space objects with arbitrary shapes reflect sunlight more or less isotropically, resulting in $P_\lambda(\theta)/4\pi \approx 1/4\pi$ (Shendeleva 2017). Substituting the approximate expressions into Eq. (4), we found for the theoretical spectral radiance in the zenith ($z = 0°$)

$$L_\lambda(z) = \frac{E_{0,\lambda} e^{-\tau_\lambda}}{2} \int_{h=h_1}^\infty \int_{r=0}^\infty r^2 \, n(r,h) \, dr \, dh. \quad (5)$$

2.2 Zenith sky luminance: An estimate

It follows from Eq. (5) that the number distribution of space objects is the only otherwise unknown quantity required to calculate these objects' contribution to total diffuse night sky brightness. We combined a number of works to estimate this function, assuming $n(r,h) = R(r)H(h)$. The function $R(r)$ models the size distribution (m^{-1}), while $H(h)$ is the number concentration of space objects (number m^{-3}). The cumulative number of LEO objects larger than a given size has been known for decades (National Research Council 1995). The rate at which the cumulative number of objects, $N(r)$, declines with increasing size is roughly constant on a log scale, which allows for the simple logarithmic approximation $\log N(r) = a \log(2r) + b$ (Fig. 3), where $2r$ is the characteristic diameter of objects in meters, and $a = -1.98$ and $b = 2.32$ are dimensionless scaling constants.

In Fig. 3, $N(r) = n_0 \int_r^{5m} R(r)dr$, where $n_0 = 1.64 \times 10^{14}$ is the dimensionless coefficient of proportionality satisfying the normalization condition $\int_{5 \times 10^{-7} m}^{5m} R(r)dr = 1$. The function $H(h)$ is scaled to satisfy the following equation

$$\int_{200km}^{1600km} 4\pi h^2 H(h) \, dh = n_0. \quad (6)$$

The integral form for $N(r)$ can be easily transformed into differential form $R(r) = -\frac{1}{n_0}\frac{dN(r)}{dr} = -\frac{a}{r \, n_0} 10^{a \log(2r)+b}$. The vertical stratification of objects in Earth orbit was modeled in accordance with Bendisch et al. (2004). We have developed an analytical formula that models the experimental data reasonably well for altitudes $h < 40000$ km (Fig. 2). Assuming h is given in metres, we found

$$H(h) = \beta \, 10^{A(\log h - D)/[B+(\log h - F)^m]-C} \quad (7)$$

with A=4.02, B=0.60, C=7.3, D=5.35, F=5.3, and m=5.32. The coefficient of proportionality, β=0.10, was derived from the normalization condition (Eq. 6).

To estimate the contribution of space objects to the diffuse brightness of the night sky at the zenith we take $E_{0,\lambda}e^{-\tau_\lambda}$ to be about $E_{0,vis} \approx 120,000$ lm m^{-2} (Al-Obaidi et al. 2014; Taleb and Antony 2020), a standard value for ground-level direct solar illuminance that is consistent with the top-of-the-atmosphere illuminance of 133,600 lm m^{-2} deduced from the 1985 Wehrli Standard Extraterrestrial Solar Irradiance Spectrum (NREL 2010; Wehrli 1985; Neckel and Labs 1981). The scattering cross-section
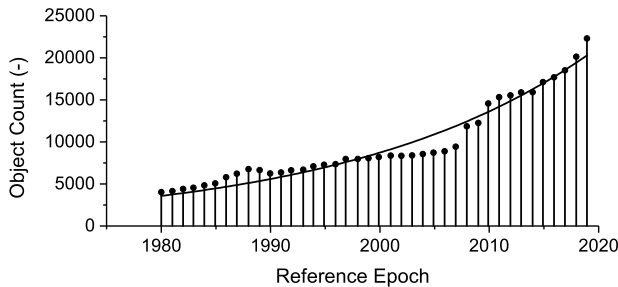
Figure 4. Trend of the absolute number of all counted space objects. Vertical lines with dots represent data provided by ESA (2020). The solid line is an analytical model.

of a spherical object asymptotically approaches $C_{sca} = \pi r^2 Q_{sca}(r)$ with the average value for all objects

$$\sigma = 2\pi \int_{5 \times 10^{-7}\ \mathrm{m}}^{5\ \mathrm{m}} r^2 R(r) dr \qquad (8)$$

and the contribution from the space objects to the zenith luminance is

$$
\begin{aligned}
L &= \sigma \alpha \frac{E_{0,vis}}{4\pi} \int_{2\times10^5\ \mathrm{m}}^{4\times10^7\ \mathrm{m}} H(h) dh \\
&= \frac{E_{0,vis}\alpha}{2} \int_{5\times10^{-7}\ \mathrm{m}}^{5\ \mathrm{m}} r^2 R(r) dr \int_{2\times10^5\ \mathrm{m}}^{4\times10^7\ \mathrm{m}} H(h) dh \\
&\approx \alpha\ 7.2\ \mu\mathrm{cd}\ \mathrm{m}^{-2},
\end{aligned}
\qquad (9)
$$

where α is the average albedo of space objects.

Due to their different shapes and orientations, the reflectivity of space objects can vary substantially. Many spacecraft are made of composite materials, much of them highly reflective for the benefit of thermal management, but other objects can appear dark because of efficient absorption. We use the average value of $\alpha \approx 0.5$ in accordance with Krutz et al. (2011).

Note that the estimate in Eq. (9) is specifically applicable to conditions during the middle to late 1990s. Based on the trend published by ESA (2020) (Fig. 4) we found that the number of known space objects has increased by a factor of 4.5 since the late 1990s. Therefore, we expect that today's contribution from space objects to zenith luminance is at least $(7.2\alpha) \times 4.5 = 16.2\ \mu\mathrm{cd}\ \mathrm{m}^{-2}$. Assuming the above increase rate remains conserved in next few years, the luminance may quickly approach $25\ \mu\mathrm{cd}\ \mathrm{m}^{-2}$ in 2030.

3 DISCUSSION

Any piece of matter in Earth orbit illuminated by the Sun reflects or scatters light, and can in principle be detected and tracked as an individual moving object if it can be distinguished from neighboring ones and its radiance is above the sensitivity threshold of one's detector. If its angular size is smaller than the instrument point-spread function (PSF), what is recorded in the image is essentially the PSF with an average irradiance directly proportional to the object radiance and inversely proportional to the PSF area. The irradiance detection threshold can be reached either by increasing the telescope numerical aperture, yielding larger irradiances, and/or by increasing the responsivity of the detector. Most

present-day instruments used for narrow-field imaging or for large astronomical surveys have enough performance as to record the individual streaks produced by many of the objects orbiting Earth, excepting those of very small sizes.

The situation is different when observing the night sky with the unaided eye. The human eye has a PSF with perceptual angular resolution of order $1'$, but it has a relatively small light sensitivity in comparison with long exposure images, even under scotopic adaptation. Except for the brighter ones, most Earth-orbiting objects cannot be visually detected and tracked individually, since their individual irradiances fall below the visual detection threshold. However, if several such objects are present within the receptive field of a retinal ganglion cell, their combined irradiance may well reach the threshold, and may be perceived as a diffuse skyglow component.

A similar diffuse skyglow effect arises when measuring the night sky brightness with highly sensitive but very low angular resolution detectors. Examples of these devices are the widely used Sky Quality Meter (SQM; Cinzano 2007) and Telescope Encoder and Sky Sensor-WiFi (TESS-W; Zamorano 2017), whose PSFs have full widths at half-maximum of $\sim 20°$. In that case the radiance of even very dim space objects may be enough to be individually detected, but the low angular resolution of the instrument unavoidably integrates the light of the many such objects present within its field of view without resolving each individual source. This results in an increased value of the diffuse night sky brightness, similar to the one that would be produced by light pollution from atmospheric scattering of the radiance emitted by anthropogenic light sources on the ground.

The estimated strength of this effect, as per direct application of Eq. (9), is currently of order $16.2\ \mu\mathrm{cd}\ \mathrm{m}^{-2}$. Note that this value was obtained from Eq. (9) by integrating the contributions of the objects located toward the observer's local zenith with a lower integration limit of 200 km, consistent with the object altitude distribution in Fig. 2 and assuming that only one half of the cross-section of the object is illuminated by sunlight as seen from the observer's position. This corresponds to the objects' phase angle at sunset or sunrise.

At the beginning or the end of the astronomical night, when the Sun is at $-18°$ with respect to the horizon, the Earth shadow reaches 328 km above the observer. Up to this orbital altitude the space objects are entirely in darkness at these moments. However, since such low-altitude orbits are relatively little populated (Fig. 2) the total number of illuminated space objects is still 99.98 per cent of the maximum. Furthermore, at that time of the night the phase angle of the objects located above the observer is $\pm72°$, so that the fraction of their illuminated surface is 0.65, instead of 0.5. The skyglow contribution of the space object cloud at the beginning and end of the astronomical night is then proportionally increased, reaching an estimated value of $21.1\ \mu\mathrm{cd}$ m^{-2}.

These luminances amount to ~ 10 per cent of the natural night sky brightness, a critical level mentioned in the 1979 resolution of the International Astronomical Union (IAU) as the limiting acceptable value of light pollution at astronomical observatory sites. According to this criterion, "...the increase in sky brightness at $45°$ elevation due to artificial

light scattered from clear sky should not exceed 10 per cent of the lowest natural level in any part of the spectrum between wavelengths 300 and 1000 nm except for the spectral line emission from low pressure sodium lamps..." (Cayrel 1979). Although the original criterion refers to the brightness at 45° elevation, it is reasonable to apply it also to zenith observations.

The concept of a 'natural level' of brightness is in itself debatable, since the natural night sky brightness in any observation band, including the visual one, is widely variable depending on the region of the sky, the location of the observer, the state of the atmosphere and the highly fluctuating strength of the airglow, as described in, e.g., Masana et al. (2021) and references therein. According to the Gaia-Hipparcos map, zenith luminance values of 200 μcd m^{-2} could be taken as a reasonable 'dark sky' luminance benchmark. A reference level of 22.0 mag arcsec^{-2} in the Johnson V band is often quoted in the literature, subject to the same variability factors as the luminance value.

Note that the true visual luminance of a Johnson $V = 22.0$ mag arcsec^{-2} sky is contingent on the arbitrarily chosen definition of the V magnitude scale (AB or Vega zero-points, Vega magnitude, etc.), and also on the spectrum of the incoming light. The same Johnson V magnitude may correspond to very different sky luminances depending on the correlated colour temperature (CCT) of the sky spectrum, as reported in Bará et al. (2020). Notwithstanding that, 22.0 Johnson V mag arcsec^{-2} corresponds to $\sim$200 μcd m^{-2} for typical sky CCTs recorded in observatories across the world (Bará et al. 2020), so both quantities can be taken as sensible and practical reference values for the brightness of the natural sky.

These results imply that diffuse night sky brightness produced by artificial space objects directly illuminated by the Sun may well have reached nowadays, and perhaps exceeded, what is considered a sustainability 'red line' for ground based astronomical observatory sites. Note that the data used in Figs. (3-4) are for detected objects only. This means the real number of objects should be even higher because, in principle, not all objects have been identified. Therefore, the above estimate is a lower limit. This effect will certainly be aggravated by the planned deployment of huge satellite 'mega-constellations' that will add a substantial number of reflecting objects in large-inclination orbits at altitudes above $\sim$ 500 km. The effect of these space objects on the diffuse brightness of the night sky is to be considered in addition to the streaks of individual objects that tend to compromise the quality of astronomical images. This is in our opinion an issue that should be taken into account by the astrophysical community in its efforts to preserve science-grade quality night skies.

The approach in this work is a first approximation to the problem, made with some simplifying assumptions. However, the results in Section 2 were derived from robust first principles and we believe they capture the basic physics of this effect. Our estimates refer only to the human visual band; estimates in other bands of the optical region, including the near-infrared, would be also informative but were not addressed in this work.

Observational campaigns to evaluate the strength of this effect should be planned and carried out. They pose an interesting methodological problem, since this new sky-glow component corresponds to a diffuse contribution slowly varying across the night sky, so no sharp borders between an affected and an unaffected area of the sky are to be expected. If these borders between adjacent patches of the sky were present, visual inspection could have been enough to detect this phenomenon: the luminance contrast of a 20 μcd m^{-2} brighter patch over a 200 μcd m^{-2} background is 0.1, well above the human detection contrast threshold for a 6° zone surrounded by a 200 μcd m^{-2} adaptation luminance field, which is 0.07 (Blackwell 1946). The lack of such sharp borders should prompt the community to make absolute measurements and compare them with models of the natural night sky and/or to monitor changes in night sky brightness on timescales of order of a few years. Comprehensive datasets of the present levels of skyglow in dark sites could provide an instrumental baseline to assess the additional contribution of the new satellite mega-constellations, and also to monitor its evolution in forthcoming years.

4 PROSPECTS AND CONCLUSIONS

The cloud of artificial objects orbiting the Earth, composed of both operational and decommissioned satellites, parts of launch vehicles, fragments, and small particles, with characteristic sizes ranging from micrometers to tens of meters, reflect and scatter sunlight toward ground-based observers. When imaged with high angular resolution and high sensitivity detectors, many of these objects appear as individual streaks in science images. However, when observed with relatively low-sensitivity detectors like the unaided human eye, or with low-angular-resolution photometers, their combined effect is that of a diffuse night sky brightness component, much like the unresolved integrated starlight background of the Milky Way.

According to our preliminary estimations, this newly recognised skyglow component could have reached already a zenith visual luminance of about 20 μcd m^{-2}, which corresponds to 10 per cent of the luminance of a typical natural night sky, exceeding in that way the IAU's limiting light pollution 'red line' for astronomical observatory sites. Future satellite mega-constellations are expected to increase significantly this light pollution source.

DATA AVAILABILITY STATEMENT

Digitized data shown in Fig. 2-4 and the numerical solvers used to model zenith NSB are publicly available on http://davinci.fmph.uniba.sk/~kundracik1/debris. We did not use any new data.

REFERENCES

Al-Obaidi K. M. et al., 2014, Front. Archit. Res. 3, 178.

Alshaibani K., 2016, Lighting Res. Technol. 48, 742.

Bará et al., 2020, MNRAS 493, 2429

Bendisch et al., 2004, Adv. Space Res. 34, 959

Blackwell H. R., 1946, J. Opt. Soc. Am. 36, 624

Cayrel R., 1979, Trans. Int. Astron. Union, 17, 215

Cinzano, P., 2007, Report on Sky Quality Meter, version L; Technical Report; ISTIL

ESA, 2020, ESA's Annual Space Environment Report, GEN-DB-LOG-00288-OPS-SD, Darmstadt, Germany

Hainaut O. R. et al., 2020, Astron. Astrophys. 636, A121.

Hergert W., Wriedt T., 2012, The Mie theory: Basics and Applications. Springer Ser. Opt. Sci. 169.

Kocifaj M., Horvath H., 2005, Appl. Opt. 44, 7378

Krutz et al., 2011, Acta Astronaut. 69, 297

Link F., 1969, Eclipse Phenomena in Astronomy. Springer.

Masana et al., 2021, MNRAS 501, 5443

National Research Council, 1995, Orbital Debris: A Technical Assessment. Washington, DC: The National Academies Press.

Neckel H., Labs D., 2011, Sol. Phys. 74, 231

NREL, 2021, 1985 Wehrli Standard Extraterrestrial Solar Irradiance Spectrum, www.nrel.gov/grid/solar-resource/spectra-wehrli.html

Shendeleva M. L., 2005, J. Eur. Opt. Soc. 13:10.

Taleb H. M., Antony A. G., 2020, J. Build. Eng. 28, 101034.

Tyson J. A. et al. 2020, Astron. J. 160, 226.

UCS 2021, Union of Concerned Scientists Satellite Database, www.ucsusa.org/resources/satellite-database

Wehrli, C. Extraterrestrial Solar Spectrum, Publication no. 615, Physikalisch-Meteorologisches Observatorium + World Radiation Center, Davos Dorf, Switzerland, July 1985.

Zamorano J. et al. 2017, Int. J. Sust. Lighting 18, 49–54.

This paper has been typeset from a TEX/LATEX file prepared by the author.